Disordered structure of D2O ice VII from in situ neutron powder diffraction

James D. Jorgensen and Thomas G. Worlton

Additional information on J. Chem. Phys.

Disordered structure of D$_2$O ice VII from *in situ* neutron powder diffraction

James D. Jorgensen

Materials Science and Technology Division, Argonne National Laboratory, Argonne, Illinois 60439

Thomas G. Worlton

Intense Pulsed Neutron Source, Argonne National Laboratory, Argonne, Illinois 60439

Neutron powder diffraction data have been collected for the ice VII phase of D$_2$O at 26 kbar and 22 °C by the time-of-flight technique. The data confirm the cubic *Pn3m* space group with completely disordered hydrogen bonding. Rietveld analysis of the data to obtain a bond length and bond angle for the D$_2$O molecule is hampered by combined static and thermal disorder of both the deuterium and oxygen atom positions. However, simple models give results which are consistent with the D$_2$O molecule parameters for other ice structures.

INTRODUCTION

At least 11 crystalline phases of ice are known to exist as a function of pressure and temperature.[1,2] Except for the most recently reported phase,[2] which exists above 440 kbar, the unit cells and space groups of all of the ice structures are known. The various structures share several common features. In all cases, the oxygen atoms are surrounded by four hydrogen atoms in perfect or nearly perfect tetrahedral directions. Two of the neighboring hydrogen atoms are covalently bonded to the oxygen atom, while the other two are hydrogen bonded. Near-neighbor oxygen atoms are, thus, linked by O–H· · ·O or O· · ·H–O bonds. The phases divide into two general groups: those in which the orientations of the H$_2$O molecules are ordered and those in which they are disordered among a finite set of possible orientations.

The high pressure phases of ice are increasingly more dense as a result of closer packing of nonbonded neighbors. The bond lengths and bond angles for individual H$_2$O molecules in the various ice phases for which precise structural measurements are available are almost identical.[3] Thus, compression occurs by reorganization of the framework into a different structure, rather than by flexibility of a given ice structure. In the higher pressure phases, ices VI, VII, VIII, high density is achieved by forming "self-clathrate" structures. These structures consist of two interpenetrating, but nonbonded, ice frameworks with each framework having the tetrahedral coordination common to the ice structures. Beyond ice VII (or ice VIII) no further densification is possible by changing the structural topology. Thus, at pressures above 21 kbar (the ice VI to ice VII transition pressure near room temperature) further compression must occur by shortening of hydrogen bonds. For this reason, it is hypothesized that the newly discovered ice X phase at 440 kbar is "symmetric ice"; a structure in which hydrogen atoms are equidistant from their two bonded oxygen neighbors.[2]

Until recently, accurate structural data for the high pressure phases of ice was limited to neutron single crystal diffraction refinements for samples of ice II,[4] V,[3] and IX[5] which were quenched from the high pressure phases and studied at atmospheric pressure. Two recent papers report *in situ* neutron powder diffraction results for ices VI, VII, and VIII.[6,7] The ice VIII structure was refined from both constant-wavelength (variable-angle) and time-of-flight (fixed angle) neutron powder diffraction data, yielding essentially identical results. The O–D bond length is 0.97 Å, and D–O–D angle is near 105°. For ice VI, the structure is sufficiently complex that the powder refinement was somewhat less precise. However, the results were consistent with other ice structures.[7]

Ice VII presents a more difficult problem in data analysis. Because the hydrogen bonding is disordered, the atom positions refined from diffraction data represent the spatially averaged atom positions (i.e., the atom positions averaged over many unit cells) which may be significantly different from the atom positions for a single unit cell. Thus, a straightforward refinement of diffraction data for ice VII can easily give misleading results unless both static and thermal displacements of the atoms are properly handled in the model. Unfortunately, static and thermal contributions to the Debye–Waller factor are difficult or impossible to separate unless the diffraction data can be extended to small d spacings (high q) and the thermal vibrations can be assumed to be harmonic. The problem is further complicated by the fact that the large Debye–Waller factors for this type of system result in greatly diminished intensity of the small d-spacing Bragg reflections.

In the *in situ* study of D$_2$O ice VII by Kuhs *et al.*, a constant-wavelength neutron powder diffractometer (D1A at the ILL) was used to collect data with the sample in a supported aluminum oxide pressure cell.[7] With this method, Bragg reflections from the aluminum oxide are unavoidable and are, in fact, larger than the desired peaks from the ice sample. Thus, the data analysis depends upon a careful "background" subtraction. Additionally, the D1A diffractometer is located on a thermal guide tube and has rapidly decreasing flux at short wavelengths. These problems limited the range of data that could be obtained. The analysis of ice VII data by Kuhs *et al.* was based on 15 Bragg intensities. Good agreement was obtained by using a model with a restricted D$_2$O molecule geometry. Useful information was gained about the (spatially and time averaged) distribution of oxygen and deuterium atoms, but it was impossible to refine an unconstrained model to probe the local O–D bond length and D–O–D bond angle of an individual molecule.

The purpose of this study is to collect a larger set of diffraction data for D$_2$O ice VII by employing the time-of-

flight technique at a pulsed neutron source. Because a fixed scattering angle can be used, scattering from the pressure cell can be eliminated with appropriate collimation of the incident and scattered beams. The pulsed neutron source offers high flux at short wavelengths and is well suited for obtaining small d-spacing data. Alternate structural models are employed in the refinement in order to illustrate what information can be obtained about the geometry of the D_2O molecule in ice VII without constraining the bond length or bond angle.

EXPERIMENTAL PROCEDURE

The D_2O sample used in this experiment was contained in a sealed Teflon capsule 7 mm o.d. and 50 mm long with a 0.3 mm wall thickness. The capsule was placed in the bore of an aluminum oxide cylinder 31.8 mm o.d. and 76.2 mm long which was supported radially by steel binding rings. The pressure cell is shown in Fig. 1. The hardened steel sleeve immediately surrounding the aluminum oxide cylinder has a tapered o.d. so that, when it is pressed into the tapered bore of the outer steel binding ring, the aluminum oxide is compressed radially to a value near its compressive strength limit. Pressure is applied to the ends of the Teflon sample tube through tungsten carbide pistons. Thus, as sample pressure increases, the compression at the inner diameter of the aluminum oxide cylinder decreases and passes through zero. The cell fails, due to fracture of the aluminum oxide, at its limiting tensile strength. The pressure cell used in this experiment is based on the early designs by Brugger et al.[8,9] and was previously used for numerous high pressure neutron diffraction measurements at Argonne's CP-5 research reactor.[10]

The ice VII data were collected on the Special Environment Powder Diffractometer[11] at Argonne's Intense Pulsed Neutron Source. Neutrons enter and leave the pressure cell through 3×28 mm windows in the hardened steel sleeve which line up with larger windows in the steel binding ring (Fig. 1). A boron nitride insert with a 2.3 mm wide slit was used in the incident beam window to provide a collimator

UPPER RAM
EXTENSION

UPPER TUNGSTEN
CARBIDE PISTON

STEEL BINDING
RING (R/C 45)

INCIDENT
BEAM

HARDENED STEEL
SLEEVE (R/C > 60)

ALUMINUM
OXIDE CYLINDER

LOWER TUNGSTEN
CARBIDE PISTON

SAMPLE

DIFFRACTED
BEAM
TO 90°
DETECTORS

TRANSMITTED
BEAM

TUNGSTEN CARBIDE

5 cm

LOWER RAM
EXTENSION

FIG. 1. Schematic of the piston-in-cylinder pressure cell used for time-of-flight neutron powder diffraction.

with higher stopping power than steel. These data were collected at a scattering angle of $2\theta = +$ and $- 90°$ where the largest possible sample volume can be viewed without unwanted scattering from the cell.

The pressure was cycled across the ice VI–VII phase boundary (21 kbar at room temperature) several times with short data collection between cycles to investigate the possibility of a nonpowder sample. No changes in ice VII Bragg intensities were observed, indicating that the sample contained a large enough number of randomly oriented crystallites to provide unbiased powder intensities. Data were also compared for the right- and left-hand 90° detector banks as a further check for large crystallites or perferred orientation. The two data sets were identical. The data used for structural refinement were collected for 67 h at a pressure of 26 kbar and a temperature of 22 °C.

Since no internal calibrant was used in the pressure cell, the determination of the sample pressure is based on a comparison of the refined lattice constant from this experiment, 3.3501(1) Å, with the equations of state given by Walrafen et al.[12] and Munro et al.[13] Since this experiment falls at the lower range of their data, error bars could be as large as ± 2 kbar. The external load on the pressure cell would suggest a somewhat lower pressure, perhaps 24 kbar. However, the sample pressure vs external load is not necessarily reproducible in this pressure cell, and the cycling of pressure up and down across the VI-VII phase line could relax piston friction and result in higher than normal pressures. Thus, the pressure should be assumed to be 26 ± 2 kbar until better equation of state data becomes available.

DATA ANALYSIS

The data were analyzed by the Rietveld technique modified for time-of-flight data from pulsed neutron sources.[14] The analysis included 35 Bragg reflections (28 independent d spacings) with d spacings from 0.54 to 2.37 Å. The refinements were done in the previously reported[1,15] cubic $Pn3m$ space group. All refinements included a four-term polynomial background function and a refineable peak width parameter.

A simple model with oxygen atoms at the special position 1/4, 1/4, 1/4, and deuterium atoms at special position x, x, x along the [111] axis, and with isotropic temperature factors for both oxygen and deuterium atoms gave an anomalously short O–D bond length of 0.93 Å. Kuhs et al. obtained an even shorter bond length (0.89 Å) for a simple model. The reason for this unlikely result can be easily understood by considering the effects of hydrogen-bond disorder in the structure.

Figure 2 shows the idealized ice VII structure. The oxygen atoms form a body-centered cubic lattice with each oxygen atom being bonded through the deuterium atoms (O–D···O or O···D–O bonds) to four of its eight near-neighbor oxygen atoms. The four nonbonded oxygen atom neighbors are part of a second interpenetrating diamond framework identical to the first. The deuterium atom positions shown in Fig. 2 each have a 50% probability of being occupied. Structural refinement is done by assigning a half atom to each allowed site to simulate the spatial average of the structure.
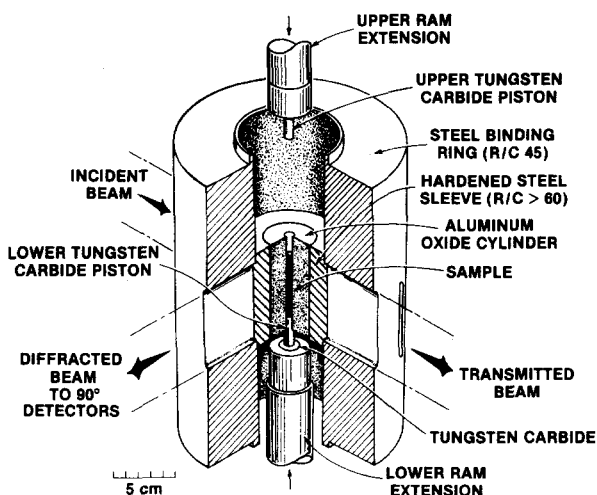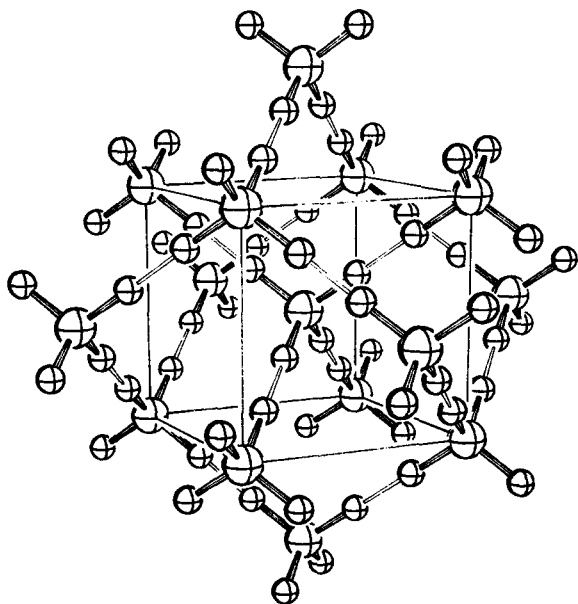
FIG. 2. The average structure of ice VII. Large spheres are oxygen atoms. Small spheres are possible deuterium atom sites which have 50% average occupancy. The cubic cell is drawn to emphasize the body-centered cubic arrangements of oxygen atoms, but does not match the cell used in the structural refinements (where the origin is at the inversion center and oxygen atoms are at 1/4, 1/4, 1/4).

On the local scale, however, each oxygen atom has two covalently bonded and two hydrogen-bonded deuterium atom neighbors. Thus, the local environment of an oxygen atom is not as symmetric as the ideal structure would imply. Rather, the near-neighbor forces on oxygen atoms would be expected to be uniaxial along the [100] directions bisecting the D–O–D bonds. The data analysis of Kuhs et $al.$ indicated the presence of these oxygen atom displacements along [100] directions and for a particular constrained model gave a magnitude for the displacement of 0.096(5) Å, which is almost equal to the distance from the oxygen atom to the center of mass of the molecule (0.12 Å).[7] Unfortunately, releasing the constraint on the O–D bond length gave an unexpectedly large value of 1.02 Å suggesting that the oxygen atom displacement may be overestimated.

The local deuterium atom positions could also differ markedly from their idealized (averaged) positions shown in Fig. 2. The D–O–D bond angle for free water vapor[3,16] and the angle that is most often observed in ice structures,[3,6,7] is near 105°, rather than the 109.5° that would correspond to perfect tetrahedral coordination. Thus, a slight folding of the D₂O molecule involving a displacement of the deuterium atoms off the [111] axes would not be unexpected. When such diplacements are averaged over molecules in all possible orientations, the $Pn3m$ symmetry is not violated and the average deuterium atom position is unchanged. A second possible displacment of the deuterium atoms could result from Coulomb attraction of the three nonbonded oxygen neighbors. Again, the average deuterium atom positions would not change.

Several possible models were tried in refinements of the D₂O ice VII data in an attempt to obtain reasonable values for the O–D bond length and the D–O–D bond angle without actually constraining the molecular geometry. In gen-

TABLE I. Structural parameters for D₂O ice VII (cubic, $Pn3m$, origin at center) for a refinement model with O at 1/4, 1/4, 1/4 and D at x, x, x. Numbers in parentheses are statistical standard deviations of the last significant digit. The temperature factor for D is defined as $\exp\{4a_0^2[- B_{11}h^2 - B_{22}k^2 - B_{33}l^2 - 2B_{12}hk - 2B_{13}hl - 2B_{23}kl]\}$.

a_0	=	3.3501(1) Å		
$B(O)$	=	2.13(6) Å²	O–D	= 0.943(2) Å
$x(D)$	=	0.4125(4) ,	D–O–D	= 109.5°
$B_{11}(D)$	=	2.57(7) Å²		
$B_{12}(D)$	=	− 0.34(4) Å²		
R_{wp}	=	2.587%		
R_{exp}	=	1.696%		

eral, these models corresponded to splitting the deuterium or oxygen atoms, or both, into partially occupied, displaced sites with either isotropic or anisotropic, harmonic temperature factors. Only the most successful and physically reasonable results are reported in this paper. It was found to be impossible to separate the oxygen atom static and thermal displacements. For models in which the oxygen atom was split into six partially occupied sites along the [100] directions, the weighted profile R value was essentially constant for static displacements up to 0.1 Å. Thus, it was impossible to draw conclusions directly from the data concerning the magnitude of displacement of oxygen atoms off their ideal positions. Subsequent refinements were done with oxygen at the special position 1/4, 1/4, 1/4 with an isotropic temperature factor.

An improved result was obtained by allowing an anisotropic temperature factor for the deuterium atoms. Table I gives the refined parameters for this model. The anisotropy of the deuterium atom distribution is pronounced. The principal axes of the thermal ellipsoid are given by

$$\langle x_\perp^2 \rangle^{1/2} = \left[\frac{1}{8\pi^2}(B_{11} - B_{12})\right]^{1/2} = 0.192(3) \text{ Å}$$

and

$$\langle x_\parallel^2 \rangle^{1/2} = \left[\frac{1}{8\pi^2}(B_{11} + 2B_{12})\right]^{1/2} = 0.155(4) \text{ Å},$$

where $\langle x_\perp^2 \rangle$ and $\langle x_\parallel^2 \rangle$ are the mean squared displacements perpendicular and parallel to the [111] axes (the O–D bond directions). The calculated bond length for this model is 0.943(2) Å and the D–O–D angle is (tetrahedral) 109.5°.

The tendency for static displacement of the deuterium atoms off the [111] axes can be tested by refining with the deuterium atom split into x, x, z positions. There are three such positions around each of the original x, x, x positions.

TABLE II. Structural parameters for D₂O ice VII (cubic, $Pn3m$, origin at center) for a refinement model with O at 1/4, 1/4, 1/4 and D at x, x, z.

a_0	=	3.3501(1) Å
$B(O)$	=	2.14(6) Å² O–D = 0.959(3) Å
$x(D)$	=	0.433(1) D–O–Dᵃ = 98.2(6)°, 100.7(4)°,
$z(D)$	=	0.373(2) 114.0(2)°, 129.0(9)°
$B(D)$	=	1.82(7) Å²
B_{wp}	=	2.561%
R_{exp}	=	1.696%

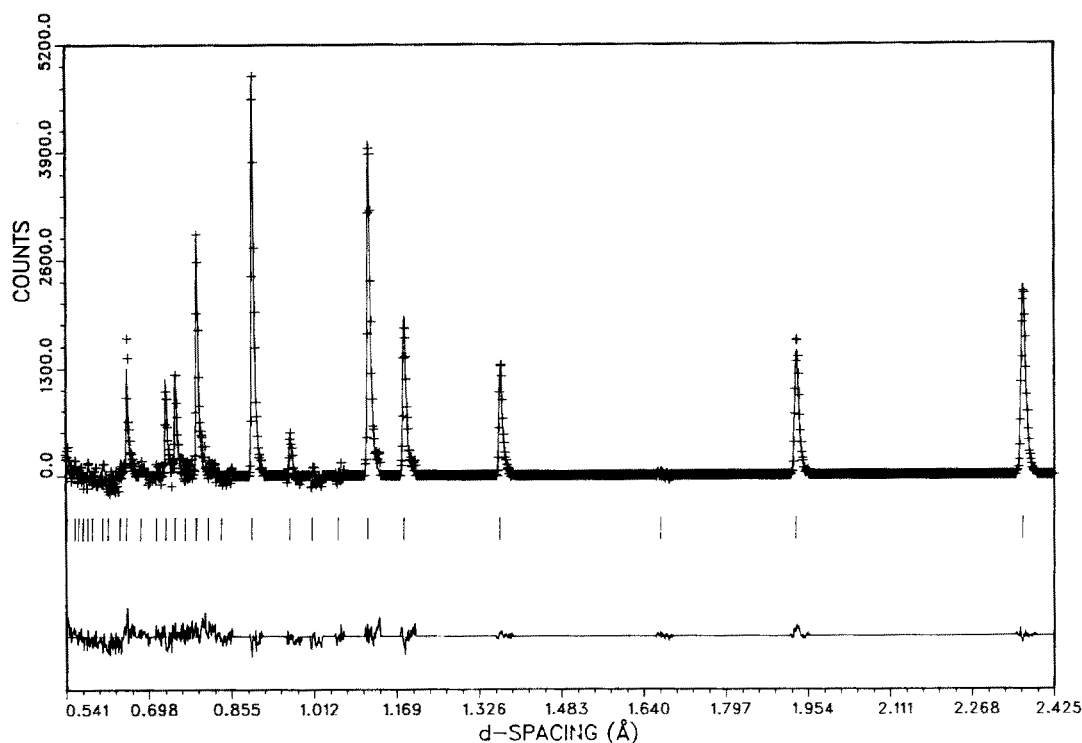ᵃ See the text for a discussion of which values are physically acceptable.

FIG. 3. Raw diffraction data (+) and Rietveld refinement profile (continuous line) for D$_2$O ice VII at 26 kbar and 22 °C for the refinement model described in Table II. Tick marks below the profile indicate the positions of allowed Bragg reflections used in the refinement. A difference curve (observed minus calculated) appears at the bottom. Background has been subtracted before plotting.

Two physically distinct cases are possible. For $x > z$, the deuterium atom displacement is toward the three nonbonded oxygen atom neighbors. For $x < z$, the three-atom distribution is rotated 60° around the [111] axis and is directed halfway between the nonbonded oxygen atom neighbors. Both cases were refined. For these models, high correlations made it impossible to simultaneously refine anisotropic temperature factors for the partial deuterium atoms in the displaced positions. Thus, isotropic temperature factors were used for both oxygen and deuterium atoms. This gives a model with the same number of parameters as that described in Table I. The results for the $x > z$ case are given in Table II. A plot of the raw data and final calculated profile is in Fig. 3. The static displacement off the [111] axis is 0.16 Å. This split atom model for $x > z$ gives a significantly lower weighted profile R value ($R_{wp} = 2.561\%$) than the anisotropic model described in Table I ($R_{wp} = 2.587$). The split atom model for $x < z$ gave a higher R value by about the same amount $R_{wp} = 2.621\%$).

These weighted profile R values are correctly defined for use in R value significance tests as presented by Hamilton,[17] where, in the powder case, the observations are counts in a given channel rather than integrated intensities. For the ice VII data analyzed in this paper, the number of "free variables" (observations minus refineable parameters) is 586. Standard R-value ratio tables can be used to test the statistical significance of various structural models.[18] For the three models used to refine the ice VII data, the split atom model with $x > z$ obtains an improvement in R_{wp} sufficient to justify up to two additional variables at the 99.5% confidence

level, when compared to the anisotropic model. Since the models actually have the same number of variables, the split atom model with $x > z$ is strongly favored by statistical tests. Thus, these results indicate a clear preference for a (static or dynamic) displacement of deuterium atoms toward nonbonded oxygen atom neighbors. The split deuterium atom model allows several D$_2$O molecule geometries as shown in Fig. 4. In all cases, the O–D bond length is 0.959(3) Å. Three of the possible bond angles are shown in Fig. 4. Based on the ice VIII structure, which is an ordered form of ice VII,[6,7] and the bond angle in the free water molecule,[3,16] the expected D–O–D angle would be near 105°. Thus, the physically reasonable molecules are those with angles less than tetrahedral (109.5°). The split atom model allows two such molecules, with angles of 98.2(6)° and 100.7(4)°.
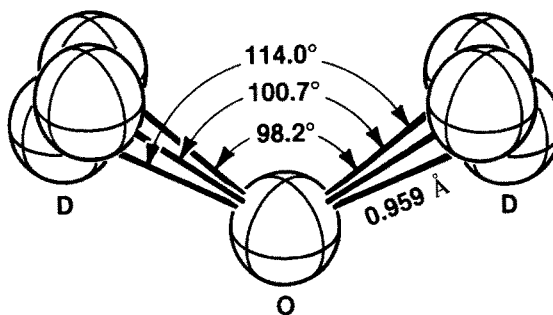

FIG. 4. Bond length and possible bond angles for the refinement model described in Table II where deuterium atoms are split into sites displaced off the [111] axis toward nonbonded oxygen atom neighbors. Each possible deuterium site has one-sixth average occupancy.

The two refinement models described in Tables I and II represent the logical extremes of the actual structure: (1) Highly anisotropic thermal motion with no static displacement or (2) isotropic thermal motion with the entire anisotropy of the density distribution being assigned as static displacement. The true situation must, of course, be somewhere between these two extremes. Thus, the bond lengths and angles from the two refinement models could be taken as upper and lower limits of the true values. Taking the mean values for the two models, the results suggest an O–D bond length of 0.95 Å and a D–O–D bond angle near 105°. Since no oxygen atom displacement has been included in these models, even though a small displacement along the [100] directions is physically expected, it is not surprising that the refined bond length is slightly shorter than the expected value (0.97 Å as in ice VIII[6,7]). Indeed, the short O–D bond length implies that a small [100] oxygen atom displacement away from the covalently bonded deuterium atoms must be present in agreement with the results of Kuhs et al.[7]

CONCLUSION

It is unlikely that unconstrained refinement of neutron powder diffraction data will be able to give more definitive structural information for ice VII than is presented in this paper and that of Kuhs et al.[7] However, both measurements indicate that the Pn3m space group is correct and that there is nothing anomalous about the D$_2$O molecule geometry in this phase of ice. A complete separation of the static and thermal components of the Debye–Waller factor requires a large number of precise data extending to the smallest possible d spacings and a more sophisticated model for the thermal motion of the deuterium and oxygen atoms and the overall molecule. The data reported in this paper suggest that powder techniques may be incapable of supplying the needed information.

The Bragg intensities diminish rapidly at small d spacings due to the large Debye–Waller factors, as can be seen in Fig. 3. This effect is not instrumental; the pulsed source technique offers high flux at short wavelengths and is well suited for obtaining data to small d spacings. In the case of D$_2$O ice VII, the limiting factor is the signal-to-noise ratio, where the background comes primarily from the deuterium incoherent scattering and from multiple scattering in the pressure cell. Improved pressure cell design and a larger sample might offer some improvement in the signal-to-noise ratio at small d spacings. However, a significantly more definitive refinement of the ice VII structure will probably not be possible unless in situ single crystal neutron diffraction data can be obtained.

[1] B. Kamb, in *Physics and Chemistry of Ice*, edited by E. Whalley, S. J. Jones, and L. W. Gold (Royal Society of Canada, Ottawa, 1973), p. 28.
[2] A. Polian and M. Grimsditch, Phys. Rev. Lett. **52**, 1312 (1984).
[3] W. C. Hamilton, B. Kamb, S. J. LaPlaca, and A. Prakash, in *Physics of Ice*, edited by N. Riehl, B. Bullemer, and H. Englehardt (Plenum, New York, 1969), p. 44.
[4] B. Kamb, W. C. Hamilton, S. J. LaPlaca, and A. Prakash, J. Chem. Phys. **55**, 1934 (1971).
[5] S. J. LaPlaca, W. C. Hamilton, B. Kamb, and A. Prakash, J. Chem. Phys. **58**, 567 (1973).
[6] J. D. Jorgensen, R. A. Beyerlein, N. Watanabe, and T. G. Worlton, J. Chem. Phys. **81**, 3211 (1984).
[7] W. F. Kuhs, J. L. Finney, C. Vettier, and D. V. Bliss, J. Chem. Phys. **81**, 3612 (1984).
[8] R. M. Brugger, R. B. Bennion, and T. G. Worlton, Phys. Lett. A **24**, 714 (1967).
[9] R. M. Brugger, R. B. Bennion, T. G. Worlton, and W. R. Meyers, Trans. Am. Crystallogr. Assoc. **5**, 151 (1969).
[10] See, for example, J. D. Jorgensen, J. Appl. Phys. **49**, 5473 (1978).
[11] J. D. Jorgensen and J. Faber, Jr., in Proceedings of the Sixth Meeting of the International Collaboration on Advanced Neutron Sources, Argonne National Laboratory Report No. ANL-82-80, 1983, p. 105.
[12] G. E. Walrafen, M. Abebe, F. A. Mauer, S. Block, G. F. Piermarini, and R. Munro, J. Chem. Phys. **77**, 2166 (1982).
[13] R. G. Munro, S. Block, F. A. Mauer, and G. Piermarini, J. Appl. Phys. **53**, 6174 (1984).
[14] R. B. VonDreele, J. D. Jorgensen, and C. G. Windsor, J. Appl. Crystallogr. **15**, 581 (1982).
[15] C. E. Weir, S. Block, and G. Piermarini, J. Res. Natl. Bur. Stand. Sect. C **69**, 275 (1965).
[16] C. W. Kern and M. Karplus, in *Water: A Comprehensive Treatise*, edited by F. Franks (Plenum, New York, 1972), Vol. 1, p. 21.
[17] W. C. Hamilton, Acta Crystallogr. **18**, 502 (1965).
[18] *International Tables for X-ray Crystallography* (Kynoch, Birmingham, England, 1974), Vol. IV; see Table 4.2, pp. 288–292.